Polysaccharide Multilayer Nanoencapsulation of Insulin-Producing β-Cells Grown as Pseudoislets for Potential Cellular Delivery of Insulin

Zheng-liang Zhi,*,† Bo Liu,‡ Peter M Jones,‡ and John C Pickup†

Metabolic Unit, King's College London School of Medicine, Guy's Hospital, London, United Kingdom, and Diabetes Research Group, School of Biomedical and Health Sciences, King's College London, Guy's Campus, London, United Kingdom

Received October 8, 2009; Revised Manuscript Received January 15, 2010

This paper describes the use of a layer-by-layer nanocoating technique for the encapsulation of insulin-producing pancreatic β-cell spheroids (pseudoislets) within chitosan/alginate multilayers. We used pseudoislets self-organized from a population of the insulinoma cell line MIN6, derived from a transgenic mouse expressing the large T-antigen of SV40 in pancreatic β-cells, as an experimental model for the study of cell nanoencapsulation. The maintenance of spheroid morphology and retention of cell viability and metabolic functionality was demonstrated postencapsulation. By depositing an additional protein-repelling phosphorylcholine-modified chondroitin-4-sulfate layer, the coatings were found to shield effectively access of large molecules of the immune systems to the antigen-presenting cell surfaces. Transmission electron microscopy analysis of the encapsulated pseudoislets revealed that the coating did not damage the cell structure. In addition, nanoencapsulation permits the cells to respond to changes in extracellular glucose and other insulin secretagogues by releasing insulin with a profile similar to that of nonencapsulated cells. These results suggest that this nanofilm encapsulation technique has the characteristics required for the efficient transplantation of cellular engineered β-cells as a cell replacement therapy for type 1 diabetes. This encapsulation method is general in scope and has implications for use in a variety of cellular therapeutics employing engineered tissues from cells generated in vitro from various sources, including those using genetic and cellular engineering techniques.

Introduction

Encapsulation of living cells such as insulin-producing pancreatic islet cells with semipermeable membranes provides added possibilities for complex cell-based therapies, promising cell transplantation without the need for immune-suppressive therapy.[1] Improved encapsulation technology of islet cells is urgently needed for the treatment of type 1 diabetes.[2] Traditional immune-isolating strategies involving the use of micro- and macro-type encapsulation approaches have used a relatively large size of capsule which imposes consequential limitations on access of cells to oxygen and nutrients and produces transplant volumes unsuitable for infusion into clinically preferred sites such as the portal bloodstream.[3,4] Recently, in an effort to reduce the size and void volume of the immune-isolation devices, several studies have introduced low transplant-volume encapsulation strategies, which include conformal microcoating,[5] surface polyethylene glycol (PEG) functionalization,[6] and more recently multilayer nanocoating.[7−10] These approaches promise optimal transplant volumes for intraportal islet transplantation and are key strategies toward improved long-term graft survival of encapsulated islet cells.

The use of nanometer-thin film buildup approaches via electrostatic layer-by-layer (LBL) assembly is particularly attractive for cell encapsulation and in vivo applications,[11] due to its mild conditions, nanoscale precision, and the ability to generate films with controlled thickness and surface characteristics.[12] Several previous studies have already demonstrated the feasibility of multilayer nanoencapsulation of human pancreatic islets using the LBL approach.[7,8] From the point of view of clinical application, however, these protocols for the encapsulated human islet transplantation suffer from primary tissue-sourcing constraints for the following reasons. An adult human pancreas contains approximately 10^6 islets ($\sim 2 \times 10^9$ β-cells), but these comprise only a minor part of total pancreatic tissue (2−3%). So islets for transplantation must be isolated from whole pancreas by enzymatic digestion, which is an inefficient process. To ensure a successful outcome, islet transplantation protocols should be able to replace up to 10^6 primary human islets per recipient, so a single transplantation may require islets from up to four donor pancreases. At present, the only suitable source of human islets for clinical use is from pancreases of heart-beating, brain-dead donors. This type of organ donor is rare, so current transplantation protocols using human islets are unlikely to make a widespread therapeutic impact on diabetes.[13]

Recent trends in transplantation therapy have put strong emphasis on alternative approaches to generating functionally competent, insulin-secreting β-cells as substitutes for donor islets, for example, by using genetic and cellular engineering techniques to produce a source of islet cells.[14−16] A number of insulin-expressing cells have been derived from insulin-secreting cell lines, non-β-cells engineered by gene therapy, β-cells from other species, and cells derived from tissue and embryonic stem cells.[13] However, a major obstacle for the clinical use of such engineered cells is their possible immunogenicity, and thus, immunoisolation appears to be a practical approach to transplantation of these cells. However, there is no suitable methodology available for encapsulating cells in the form of in vitro

* To whom correspondence should be addressed. E-mail: z.zhi@kcl.ac.uk.
† King's College London School of Medicine.
‡ School of Biomedical and Health Sciences.

10.1021/bm901152k
Published on Web 01/28/2010

engineered artificial tissues or organs using the clinically preferred low transplant-volume nanoencapsulation technologies.

The insulinoma cell line MIN6 is a convenient insulin-producing cell source that has been traditionally used as an experimental model for studying the mechanism of glucose-stimulated insulin secretion in pancreatic β-cells.[17] MIN6 cells have been previously used in a microencapsulation system[18,19] and shown to reverse diabetes in rats.[19] Dispersed single MIN6 cells are, however, unsuitable for encapsulation in a nanocoating with a low void volume, because they may rapidly undergo apoptosis due to lack of cell-to-cell interactions that are needed also for maintaining normal functions including glucose-dependent secretion of insulin in MIN6 cells.[20] Nevertheless, it is well-known that individual MIN6 cells dispersed into cell suspensions can spontaneously reaggregate in vitro into three-dimensional islet-like structures ("pseudoislets") that support cell viability and restore some of the function lost on tissue dispersal.[21,22] In accordance with this, in the present study we have prepared pseudoislet structures by taking advantage of a self-organization process of the individual MIN6 β-cells in culture and then used the LBL multilayer build-up approach to develop an encapsulation methodology for the artificial tissue. We introduced a phosphorylcholine (PC)-modified sulfated glycosaminoglycan as the outermost layer in an effort to provide enhanced biocompatibility of the nanocoating. This method opens the route toward immunoisolating encapsulation for in vitro-generated cells that may potentially form the basis for future treatments for diabetes and other diseases by immune-protected therapeutic cell transplantation.

Experimental Section

Materials. Tissue culture reagents, including Dulbecco's modified Eagle's medium (DMEM), glutamine, penicillin, streptomycin, phosphate-buffered saline (PBS), fetal bovine serum, trypsin-ethylenediaminetetraacetic acid (EDTA), tolbutamide, and phorbol myristate acetate (PMA), were from Sigma-Aldrich. Chitosan (low molecular weight, 50−190 kDa, 75% deacetylation; the charge density of chitosan is directly related to the degree of deacetylation) and alginic acid sodium salt from crown algae, viscosity of 2% solution at 25 °C, ~250 cps, molecular weight, 75−100 kDa, and chondroitin-4-sulfate (20 kDa) were also from Sigma-Aldrich. Antimouse-MHC Class I antibody (MCA 2189) was purchased from AbD Serotec (MorphoSys US Inc.). The fluorescence CellTiter-Blue cell viability assay was purchased from Promega (Hampshire, U.K.).

Fluorescence Labeling of Chitosan. Chitosan (2 mg) taken from the 1% (W/V) stock solution was diluted to 1 mL in 10 mM HEPES, pH 7.4. Alexa Fluor 647 carboxylic acid succinimidyl ester (Invitrogen, Eugene, U.S.A.; 1 mg) was dissolved in 1 mL dimethylsulfoxide (Sigma). An aliquot (0.1 mL) of the dye was added to the saccharide solution and mixed thoroughly overnight at 4 °C on a rocking platform. The resulting solution was dialyzed for 16 h against 10 mM Tris, pH 7.4, to remove excess dye and stored at 4 °C in the dark until needed for encapsulation experiments.

Preparation of PC-Modified Chondroitin-4-sulfate. PC-glyceraldehyde was prepared by the procedure reported by Miyazawa and Winnik.[23] Hydrazide derivatization of chondroitin-4-sulfate was prepared by the procedure described below. Chondroitin-4-sulfate (100 mg) and carbohydrazide (40 mg) were mixed in formamide (10 mL), and sonicated for 10 min to dissolve the solids completely. 1-Ethyl-3-[3-dimethylaminopropyl]carbodiimide hydrochloride (EDC; Sigma; 90 mg) was then added, and the reaction mixture was stirred at ambient temperature for 6 h; the reaction product was purified by dialysis (membrane of MWCO 10000) against 10 mM phosphate buffer, pH 7.4, for 2 days. The PC-modified chondroitin-4-sulfate with a PC content of one PC per two disaccharide units was synthesized by the hydrazone formation and reduction amination (see Scheme 1). The procedure is described below briefly. A solution of PC-glyceraldehyde (0.10 g) in methanol (2 mL) was added dropwise to the solution of hydrazide derivatized chondroitin-4-sulfate (the dialyzed solution of about 15 mL). The reaction mixture was stirred for 30 min at 0 °C and adjusted the pH to 8.5 by adding aqueous NaOH (0.1 M). The solution was then added dropwise a solution of sodium cyanoborohydride (0.10 g) in water (1 mL) under stirring at 0 °C and was stirred continuously overnight at room temperature. The reaction mixture was dialyzed (membrane of MWCO 10000) against phosphate buffer and then water for 2 days. The white fiber-like PC-chondroitin-4-sulfate was obtained by lyophilization (yield ca. 0.15 g). ^{1}H NMR (D_2O, δ): 2.90 ppm (9H, $-N^+(CH_3)_3$), 3.30 ppm (2H, $-CH_2-N^+-$). For detailed NMR spectra, see Supporting Information.

Scheme 1. Synthesis of Phosphorylcholine-Modified Chondroitin-4-sulfate

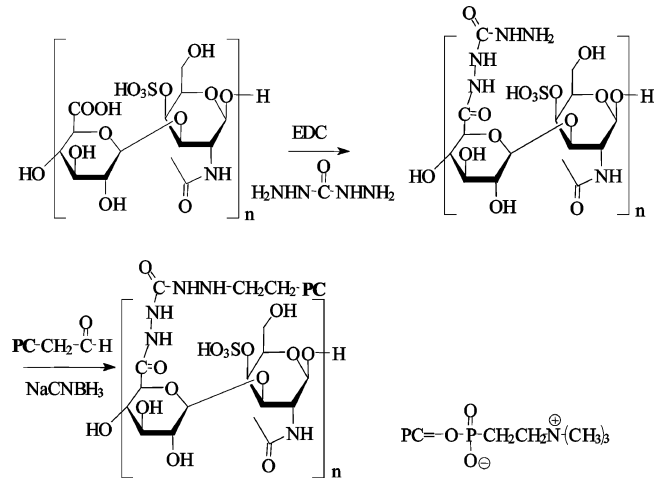

Maintenance and Preparation of MIN6 Cells. MIN6 β-cells (passage 27−38) were maintained at 37 °C (95% O_2/5% CO_2) in DMEM supplemented with 15% fetal calf serum, 2 mM glutamine, and 100 U/mL penicillin with 0.1 mg/mL streptomycin. The medium was changed every 3−4 days, and the monolayer cells were trypsinized (0.1% trypsin, 0.02% EDTA) for experiments when 80−90% confluent.

Preparation of MIN6 Pseudoislets. MIN6 pseudoislets were formed by culturing MIN6 cells in 90 mm bacterial (uncoated) Petri dishes under the same conditions as described above for monolayer cells. After 6−8 days of subculturing, each Petri dish contained at least 500 MIN6 pseudoislets with a diameter of about 100 μm (Figure 1). The pseudoislets formed were sufficiently robust to be handled with glass or plastic micropipets. During the subculture, some cells die and are released from the pseudoislets into the culture medium, so the medium was changed every 3−4 days to remove the suspended dead cells.

Encapsulation of Islet Cells. Low molecular weight chitosan (0.2 g) was dissolved in 1% acetic acid to give a stock solution of 1% (W/V). An alginate stock solution (1%) was prepared in water. The working solutions of the polysaccharides (1 mg/mL) were prepared by diluting the stocks in PBS (pH 7.20), with 2 mM Ca^{2+} supplemented because pseudoislet formation was reversible and dependent on extracellular Ca^{2+}.[21] Oppositely charged chitosan and alginate were alternatively self-assembled into a multilayer film on MIN6 pseudoislets in successive adsorption steps. After removing the medium from cells, cationic chitosan (200 μL) was added first to the cells (the cell surface is negatively charged) to initiate film growth on the cell surfaces. After a 5 min deposition time, excess unadsorbed chitosan was removed and cells were washed twice with 0.5 mL PBS, using gravity sedementation for 1−2 min. Subsequently, the anionic alginate (200 μL) was adsorbed in the same manner to form a single chitosan/alginate bilayer. This process was repeated until a desired layering scheme of cells/(chitosan/alginate)$_n$ chitosan was produced, where n represents the number of bilayers. A protein-repelling PC-chondroitin-4-sulfate was further

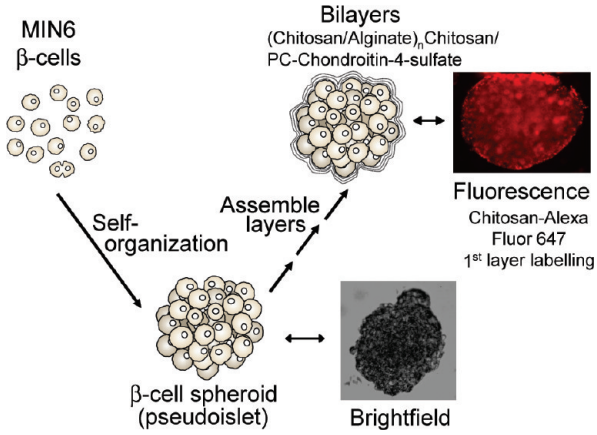

Figure 1. Illustration showing formation of pseudoislets from MIN6 β-cells and the LBL nanofilm encapsulation of the pseudoislets in multilayer coatings. The right-side image was obtained by coating a layer of fluorescence-labeled chitosan. The light micrograph (the lower frame) shows the morphology (~100 μm in diameter) of a typical pseudoislet used for nanoencapsulation.

deposited as the outermost layer of the coating, making the surface highly hydrophilic to help reduce nonspecific host responses (e.g., fibroid formation) during subsequent transplantation of the capsules. All encapsulations were performed in a tissue culture hood, and solutions used for cell encapsulation were filtered through a sterile 0.2 μm membrane filter cartridge. The encapsulated pseudoislets were visualized using Hitachi H7600 transmission electron microscope (TEM) after fixing, sectioning and staining.

In Vitro Stability Tests. The stability of pseudoislet cells postencapsulation was studied by maintaining the encapsulated cells in culture medium for 7 days and examining the morphology of pseudoislets with different layer numbers by microscopy.

Cell Survival in Culture. The long-term cell survival in culture was tested by a two-color fluorescence viability test involving the use of propidium iodide (PI) and fluorescein diacetate (FDA).[24] The staining process involved removing medium from cells, adding working solutions of PI/FDA to cells containing 2 pg of FDA plus 0.6 pg of P1 in 0.2 mL, resuspending the cell suspension, and incubating for 3 min at room temperature. This was followed by removing the staining solution and washing cells with 0.5 mL of PBS three times. The cells were then viewed under a fluorescence microscope with 478−495 nm and 530−560 nm excitation filters and 510−555 nm and 573−648 nm emission filters, respectively. This allowed green (alive) and red (dead) fluorescing cells to be viewed separately. The cell survival test experiments were carried out after two and five weeks of culturing.

Antibody Exclusion Assay. An antibody exclusion assay was used to test the permeability of the nanofilm capsules to large molecules. FITC-labeled antimouse major histocompatibility antigens (MHC) Class I antibody, with a molecular weight of 150 kDa, which targets MHC Class I antigens displayed on beta-cell surfaces was used. Antibody-FITC (1 mg/mL) in PBS was prepared and kept at 4 °C until used. Pseudoislets (encapsulated) were incubated at 37 °C in the culture medium (10 mL). To 90 μL of the cell suspension, 10 μL of normal mouse serum (Invitrogen) was added as the blocking agent, and then 1 μL of antibody-FITC solution was added. The solution was then placed on an agitator plate for 30 min. The pseudoislets were then rinsed twice with PBS-Tween (0.5 mL) to remove all unbound dye. Naked and encapsulated pseudoislet cells were then transferred to a coverslip for observation with a fluorescence microscope.

Insulin Secretion: Static Incubations. Encapsulated and naked pseudoislets were aliquoted (in 0.08 mL suspension) in quadruplicate into 0.5 mL Eppendorf tubes at a density of about 30 islets/tube. After sedimentation of the cells, the buffer was removed and 0.5 mL solution added containing (1) 2 mM glucose, (2) 20 mM glucose, (3) 20 mM glucose plus 500 nM PMA, (4) 20 mM glucose plus 100 μM tolbutamide, or (5) 20 mM glucose plus 100 μM tolbutamide and 500 nM PMA, all prepared in a bicarbonate-buffered physiological salt,[25] supplemented by 2 mM $CaCl_2$ and 0.5 mg/mL bovine serum albumin (BSA). The cells were then incubated for 30 min at 37 °C (95% O_2/5% CO_2). The insulin content of the incubation media (0.1 mL) was assessed in duplicate by a standard radioimmunoassay.[26] Statistical analysis for the determination of differences in the measured properties between groups was assessed by Bonferroni's *t*-test for multiple comparisons. Differences were considered to be statistically significant when the *p* values were less than 0.05.

Results and Discussion

Selection of Coating Materials. Previous studies have investigated LBL multilayer coating for living cells using synthetic polymers like poly(styrene sulfonate) and poly(allylamine hydrochloride), a polyanion and a polycation, respectively,[7,9] but these were found to be highly cytotoxic,[8] and are thus not generally suitable for the envisaged biomedical applications. We chose here positively charged chitosan and negatively charged alginate for the coating materials due to their similarities with the extracellular matrix, chemical versatility, as well as typically good biological performance (biocompatibility).[27] Chitosan is a natural, linear cationic polysaccharide comprised of randomly distributed β-(1−4)-linked D-glucosamine and *N*-acetyl-D-glucosamine. The anionic alginate is also a polysaccharide linear copolymer with homopolymeric blocks of L-guluronic and D-mannuronic acid covalently linked in different sequences or blocks. Both saccharides have been investigated for use in entrapping cells into beads and other shapes in tissue-engineering scaffolds which may enhance cell survival and growth.[28,29] However, the thickness of the alginate or alginate/chitosan gel formed typically by interactions between alginate and Ca^{2+} as those used in microencapsulation, was usually in the range of tens to a few hundred μm, which is much thicker compared to the LBL multilayer films as prepared in this work (in tens nm). In this work, we have assessed the cytotoxicity of chitosan and alginate in LBL coatings and the data will be discussed later. We also tested a PC-modified chondroitin-4-sulfate as the outermost layer of the coating in order to reduce nonspecific protein adsorption of the chitosan/alginate nanofilm. The polymers containing the PC moiety are of particular interest for biomaterials applications in view of the remarkable protein-repelling properties and hemocompatibility of the functional group.[30] We prepared PC-modified chondroitin-4-sulfate using a route whereby PC groups were conjugated via PC-glyceraldehyde to a preformed carbohydrazide-derivitized chondroitin-4-sulfate by reductive amination, which was in a way similar to that of the preparation of PC-chitosan first proposed by Miyazawa and Winnik.[23]

MIN6 Pseudoislet Formation and Nanofilm Coating. Due to their capacity for propagation in culture in vitro, we used mouse insulinoma MIN6 cell pseudoislets as an experimental model for the study of β-cell nanoencapsulation methodology. Previous studies showed that dispersed beta-cells are poorly responsive to insulin secretagogues due to loss of homotypic β-cell interactions within islets that are crucial for normal function.[20] MIN6 cells grown as adherent monolayers are also poorly responsive to glucose and other stimuli. However, their secretory responsiveness is greatly increased when the cells are grown as three-dimensional islet-like structures (pseudoislets) in vitro.[20,21] The pseudoislets were formed from MIN6 cell suspensions subcultured in a Petri dish, where the cells did not adhere to the plastic substrate but developed into three-dimensional cell clusters (Figure 1). The MIN6 pseudoislets

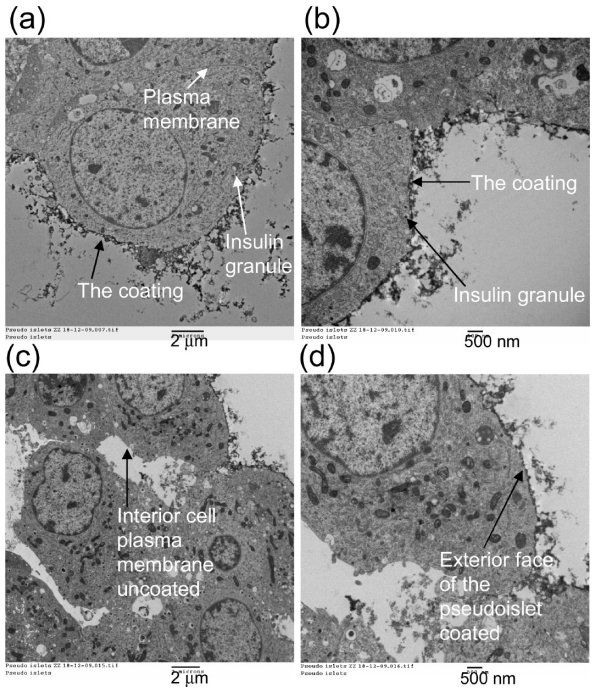

Figure 2. TEM images of the sectioned encapsulated pseudoislets. All psedoislets were coated five bilayers comprising (chitosan/alginate)$_4$ chitosan/PC-chondroitin-4-sulfate. (a,b) Different magnifications of the nanocoated pseudoislets. (c,d) Cell plasma membranes inside a pseudoislet were uncoated while the exterior faces of the pseudoislet were well-coated.

reached a diameter of about 100 μm and an appearance similar to that of primary rodent islets, and contained a cell content of 3000−5000 cells/pseudoislet after 6−8 days of subculturing.[20]

Pseudoislets were coated with a multilayer of alternating chitosan and alginate using a LBL process with the first layer being positively charged chitosan. The deposition of the layer on cell surfaces was confirmed by depositing a layer of chitosan labeled with Alexa Fluor 647 (Figure 1). The addition of the fluorescent chitosan layer to the cell suspension resulted in strong fluorescence localized mainly on the face of cells at the pseudoislet periphery, indicating successful coating. Note due to the nanothickness of each layer, it is impossible for an optical microscope to resolve whether the islet was fully covered by the layer or not. By comparing the fluorescence intensity of the coatings obtained by using fluorescence-labeled chitosan as the first, third, and fifth layer, respectively, we found that the third and fifth steps adsorbed the material in greater quantities than the first step (data not shown). This is likely due to the limited surface charge on the cell surfaces which resulted in restricted initial polyelectrolyte coating, but the polysaccharide seeding layer significantly improved the subsequent layer deposition. This could be explained that one or both of the polyelectrolytes diffuse within the initial film during each adsorption cycle, leading to an exponentially growth of the multilayers.[31] The multilayer deposition on cell surfaces was monitored and confirmed by electrokinetic zeta-potential measurements (Supporting Information). The average thickness of each dried layer, according to our previous estimation, was about 1.5 nm.[32]

The deposition of the polysaccharide nanofilms on the pseudoislets was further confirmed by TEM imaging of the sectioned encapsulated pseudoislets, as shown in Figure 2. The images of the pseudoislets showed the coating multilayers were located continuously around the exterior faces of the pseudoislets, and the interior part of the cell plasma membrane was uncoated, indicating the pseudoislets were coated in bulk. Meanwhile, the insulin secreting vesicles were aligned along the plasma membrane ready for exocytosis, and the nuclei showed no sign of apoptosis, suggesting the beta cells were healthy and unaffected by the coating. In (a), the cell plasma membranes at the MIN6 cell−cell interfaces can be seen.

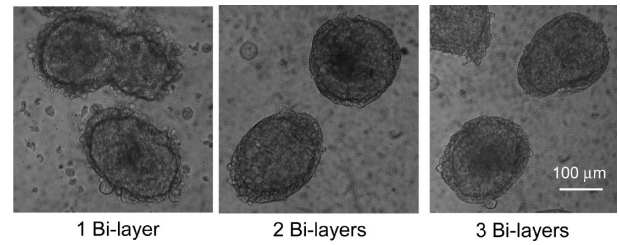

Figure 3. Light microscopy images showing capsule stability in culture medium as a function of number of bilayers coated.

Maintenance of Morphology of the Pseudoislet. Multilayer-coated pseudoislets exhibited better mechanical robustness than the naked ones, as indicated by an increase of about 50% in cell volume after three bilayers were deposited. This can be explained by the cells becoming mechanically stronger after the encapsulation, so they cannot be packed as densely as the naked ones, therefore, occupying more volume. The stability of the coated pseudoislets was evaluated in vitro by maintaining the three-dimensional cell capsules in culture medium at 37 °C for up to 7 days after encapsulated with different numbers of chitosan/alginate bilayers. Capsule stability was measured by monitoring the changes in pseudoislet morphology and release of the dead cells from the formed pseudoislets. As can be seen in Figure 3, in a coating with one chitosan/alginate bilayer, some cells were released from the pseudoislets, suggesting that a single bilayer was not stable enough to maintain the configuration or mechanical integrity of the pseudoislets, possibly due to incomplete coverage of the coating on all area of the pseudoislet. However, cells coated with (chitosan/alginate)$_2$ and (chitosan/alginate)$_3$ bilayers exhibited a stable coating and spheroid configuration, with all the cells being retained in the capsule over 7 days in culture. In subsequent experiments the capsules were found to be essentially stable for up to five weeks postencapsulation.

Cytotoxicity of the Coating Materials. The cytotoxicity of the coating materials in coating was assessed using the CellTiter-Blue cell viability assay, according to the recommended Promega protocol. The viability assay is based on the ability of living cells to convert a redox dye (resazurin) into a fluorescent end product (resorufin). As shown in Figure 4, coatings of either a chitosan single layer, or (chitosan/alginate)$_n$ multilayers resulted in no significant deleterious effect on the cell viability when compared to nonencapsulated control pseudoislets when the layers were deposited at pH 7.2 ($p > 0.05$). Exposure of nonencapsulated control pseudoislets to a medium at pH 5.5 had no detectable effect on cell viability. However, a significant decrease in the cell viability was observed when coating was performed at this pH ($p < 0.05$ for the first coating, and $p < 0.01$ for successive coatings), and the degree of cytoxicity at pH5.5 was dependent on the number of layers deposited (Figure 4).

Long-Term Viability of the Encapsulated MIN6 Cells in Culture. After maintenance in culture medium for various time periods, the survival of encapsulated cells within three bilayers was assessed using a two-color fluorescence cell viability assay with the cell-permeable esterase substrate FDA and the cell impermeant nucleic acid stain PI (green fluorescence

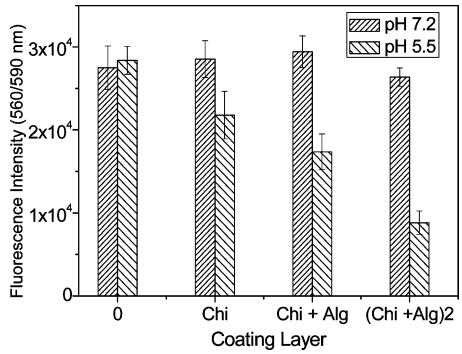

Figure 4. Cytotoxicity of the coating materials toward the MIN6 β-cells: effect of coating materials and number of layers on the viability of the encapsulated pseudoislets, studied at pH 7.2 and 5.5. Chi = chitosan; Alg = alginate.

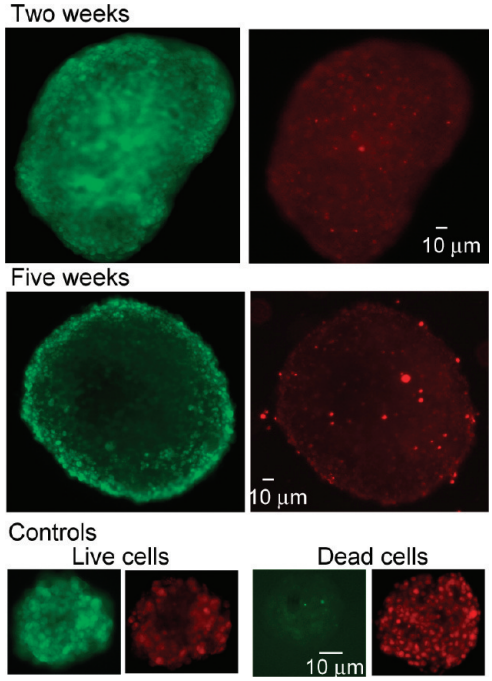

Figure 5. Live/dead MIN6 cells encapsulated within three bilayers of chitosan/alginate after a 14 (top panel) and a 35 (middle panel) day postencapsulation maintained in tissue culture. The lower panels show the controls of the viable and dead cells (nonencapsulated). Green: viable; red: nonviable. CS-PC = phosphorylcholine-substituted chondroitin-4-sulfate.

indicates the cells being viable, and red indicates the cells dead). Living cells in a pseudoislet grown in the media for 7 days was used as the positive control, and dead pseudoislet cells were obtained by treating the viable cells with 50% PEG200 for 30 min. As shown in Figure 5, most of the cells, particularly those located near the edge of pseudoislet were viable after two weeks of culturing. After five weeks, there were a few more dead cells, but the majority were still viable. Note, due to the 3-D nature of the pseudoislet, not all of the cells in the pseudoislet could be visualized at once using a conventional fluorescence microscopy. The long survival period of the encapsulated cells in culture suggested again that the pseudoislet was more likely encapsulated in bulk, but not just only some individual cells coated. This is because cells coated individually are physically isolated each other and may rapidly undergo apoptosis and eventually die due to lack of cell-to-cell interactions. An unimpaired glucose-dependent insulin secretion and release of the encapsulated β-cells, as described below, further support this argument.

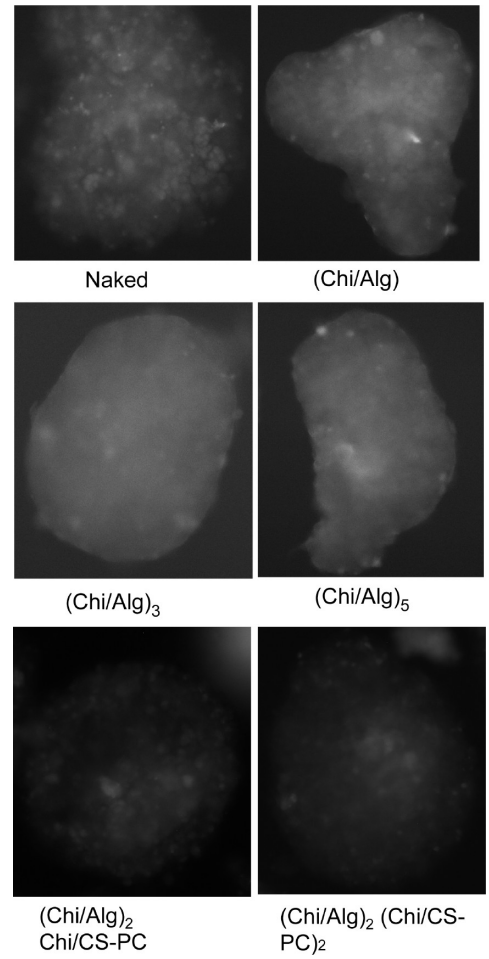

Figure 6. Fluorescence images of MIN6 β-cells showing the penetration or exclusion of anti-MHC-FITC by the chitosan/alginate and chitosan/alginate/phosphorylcholine-substituted chondroitin-4-sulfate multilayers. The size of each pseudoislet is around 100 μm.

Exclusion of Large-Molecule Access to the Multilayer-Coated Cell Surfaces. Effective immunoisolation requires that the multilayer coating excludes the much larger components of the immune system, including antibodies and lymphocytes that would cause rejection and destroy the implant. The ability to exclude antibodies, which are approximately 150 kDa in size, is determined by the thickness and density of the coating, typically achieved via size selection with nanopores of <10 nm. We used an antibody against MHC Class I antigens to demonstrate the exclusion of macromolecules. MHC antigens are a set of plasmalemmal glycoprotein antigens involved in graft rejection and other immune phenomena, and include two classes of cell-surface glycoproteins, referred to as class I and II MHC molecules.[33] The antibody used here binds specifically to the MHA class I expressed on the surface of mouse β-cells. After fluorescence immunoctyochemical staining, fluorescence microscopy was used to determine the binding of the antibody to the β-cell surface.

We varied the number of layers in the coatings in an effort to study the effect of film thickness on macromolecule exclusion. As shown in Figure 6, a naked islet (upper left panel) showed clear binding of the antibody-FITC probe to the surface of individual cells within the pseudoislets structures. The image of a one-bilayer-coated pseudoislet (upper right panel) shows partial exclusion of the antibody probe, indicating incomplete film coating, consistent with that observed in stability tests. In contrast, two- or three-bilayer-coated pseudoislets (middle

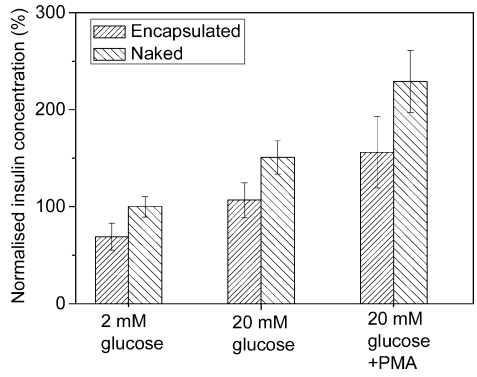

Figure 7. Insulin release of the control (naked) and encapsulated MIN6 pseudoislets in response to nutrient and non-nutrient stimuli. Insulin release into the incubation medium was normalized against basal (2 mM glucose) secretion from control pseudoislets. Each observation used about 30 pseudoislets, and bars show means ± SEM values for four independent observations, each of which was assayed in duplicate for the insulin content.

panels) showed clear exclusion of the antibody probe from access to the cell surface. However, low levels of fluorescence were detected around the periphery of the capsules surrounding the clusters, suggesting some nonspecific antibody adsorption on the nanofilm that may potentially induce fibrotic overgrowth on the capsule. To minimize the nonspecific binding of the antibody, we tested further deposition of a protein-repelling biopolymer PC-chondroitin-4-sulfate on the top of (chitosan/alginate)$_2$chitosan multilayers. As shown in Figure 6 (the lower panels), deposition of one or two layers of chondroitin-4-sulfate-PC reduced strongly the antibody adsorption on the surfaces.

Insulin Secretion from Encapsulated Pseudoislets. We investigated whether the nanofilm coatings affected the function of the beta-cells and whether the nanocoating permits the passage of small molecules like insulin (MW 5.7 kDa), glucose and oxygen through the coating film. We measured the release of insulin from coated and naked control pseudoislets in response to glucose (2 vs 20 mM) and a non-nutrient stimulator of insulin secretion, the protein kinase C activator, PMA (500 nM).[34] As shown in Figure 7, the basal rate of insulin release into the medium at a substimulatory glucose concentration (2 mM) was similar for both naked and encapsulated cells. Note the original basal concentration in the medium was 0.75 ng/mL after a dilution factor of 1 to 5. Increasing the glucose concentration to a maximum stimulatory concentration (20 mM), significantly enhanced insulin secretion from both control and encapsulated pseudoislets ($p < 0.01$), and this glucose-induced insulin secretory response was further enhanced by the presence of PMA (500 nM).

Under all conditions tested, the overall mass of insulin released from encapsulated cells was ~20−30% less than from nonencapsulated control cells. This could not be attributed to differences in insulin content, because our direct measurements of insulin in cell extracts found no significant differences between control and encapsulated cells, consistent with the viability of the encapsulated pseudoislet cells (Figures 4 and 5). We therefore considered whether the reduced rate of insulin release from encapsulated cells was due to impaired β-cell function, or to the mass diffusion limitations of the nanofilm. When the data for insulin secretion (Figure 7) were expressed relative to the appropriate basal rate of secretion (2 mM glucose) the magnitude of the secretory responses induced by glucose and PMA were very similar between control and encapsulated pseudoislets (controls: 20 mM glucose 151 ± 18% basal, mean ± SEM, $n = 4$; 20 mM glucose plus 500 nM PMA, 229 ± 32% basal; encapsulated: 20 mM glucose 155 ± 18% basal; 20 mM glucose plus 500 nM PMA, 226 ± 37% basal). These observations suggest that the encapsulation process did not impair the ability of the cells to respond appropriately to glucose nor influence the enhancement of glucose-induced insulin secretion by a non-nutrient secretagogue, such as PMA. This conclusion was confirmed in further experiments in which we used the sulphonylurea drug, tolbutamide, to induce insulin secretion. The sulphonylureas bypass the glucose-regulated stimulus-response pathway by interacting directly with ATP-sensitive K^+ (K_{ATP}) channels in the β-cell plasma membrane to induce depolarization, with the consequent influx of extracellular Ca^{2+} and initiation of the exocytotic release of insulin.[35] Although its mode of action ensures that tolbutamide activates all the β-cells within the pseudoislets, the secretory responses to tolbutamide (100 μM) were similar to those induced by glucose and PMA, with encapsulated cells releasing less insulin than control cells (~20%). However, the magnitude of the tolbutamide-induced response over basal was similar between encapsulated and control cells, consistent with the encapsulation process imposing a mass transport limitation for secreted insulin diffusing through the standard three-layer nanofilm (controls: 100 μM tolbutamide, 161 ± 23% basal, mean ± SEM, $n = 4$; 100 μM tolbutamide plus 500 nM PMA, 265 ± 12% basal; encapsulated: 100 μM tolbutamide, 183 ± 19% basal; 100 μM tolbutamide plus 500 nM PMA, 248 ± 12% basal). Furthermore, increasing the encapsulation process to five bilayers was found to not further significantly impede insulin release into the medium, while pseudoislets encapsulated with only one bilayer showed insulin secretory responses similar to the nonencapsulated cells (data not shown).

In summary, our measurements of insulin secretion from encapsulated pseudoislets demonstrate that the encapsulation methodology did not compromise the ability of the MIN6 cells to recognize and respond to changes in the extracellular concentration of nutrient stimuli, such as glucose; to non-nutrient stimuli, such as PMA or to depolarizing pharmacological agonists such as tolbutamide. These observations confirm the metabolic and secretory viability of the encapsulated β-cells in pseudoislets and suggest that this method of encapsulation is compatible for maintaining the secretory function of transplanted islets.

Conclusions

By using pseudoislets formed from MIN6 β-cells as an experimental model, we have demonstrated the feasibility of a polysaccharide nanoencapsulation methodology for islet-like β-cell spheroids. The preservation of cellular metabolism of the cells postencapsulation and efficient exclusion of antibodies to the capsule was demonstrated and suggested this nanofilm encapsulation technique has the characteristics required for improved transplantation of insulin-producing cells. A PC-modified chondroitin-4-sulfate layer was found to be an effective way of developing biocompatible surface coatings of controlled protein adsorption properties. This work establishes the basis for a versatile approach for encapsulating cell clusters formed from isolated single cell suspensions. While the MIN6 cells used in this study may not match exactly the insulin secretory kinetics of normal human or animal islets, therefore, not necessarily being compatible with the transplantation models, the methodology using self-organized pseudoislets is generic and has important implications for use in a variety of in vitro-generated

cellular therapeutics where technological and immunological barriers to cell transplantation exist. In future research, it will be necessary to further optimize the nanocoatings using an in vivo transplantation animal model with a view to obtaining significantly improved long-term survival of the transplanted cells.

Acknowledgment. The authors acknowledge the EPSRC (EP/D062861/1) for generous grant support. The MIN6 pseudoislet model was developed using grant support from the NC3Rs. We thank Dr. Faaizah Khan, Dr. Tania Saxl, and Matteo Ferla for valuable discussions.

Supporting Information Available. (1) ^{1}H NMR spectra of (a) phosphorylcholine-modified chondroitin-4-sulfate and (b) chondroitin-4-sulfate in D_2O; (2) Zeta potential of the naked and coated MIN6 islet cells. This material is available free of charge via the Internet at http://pubs.acs.org.

References and Notes

(1) Wilson, J. T.; Chaikof, E. L. *Adv. Drug Delivery Rev.* **2008**, *60*, 124–45.
(2) Pickup, J. C.; Zhi, Z.-L.; Khan, F.; Saxl, T.; Birch, D. J. S. *Diabetes Metab. Res. Rev.* **2008**, *24*, 604–10.
(3) Beck, J.; Angus, R.; Madsen, B.; Britt, D.; Vernon, B.; Nguyen, K. T. *Tissue Eng.* **2007**, *13*, 589–98.
(4) Koo, S. K.; Kim, S. C.; Wee, Y. M.; Kim, Y. H.; Jung, E. J.; Choi, M. Y.; Park, Y. H.; Park, K. T.; Lim, D. G.; Han, D. J. *Transplant. Proc.* **2008**, *40*, 2578–80.
(5) Wyman, J. L.; Kizilel, S.; Skarbek, R.; Zhao, X.; Connors, M.; Dillmore, W. S.; Murphy, W. L.; Mrksich, M.; Nagel, S. R.; Garfinkel, M. R. *Small* **2007**, *3*, 683–90.
(6) Lee, D. Y.; Yang, K.; Lee, S.; Chae, S. Y.; Kim, K. W.; Lee, M. K.; Han, D.-J.; Byun, Y. *J. Biomed. Mater. Res., Part A* **2002**, *62*, 372–77.
(7) Krol, S.; del Guerra, S.; Grupillo, M.; Diaspro, A.; Gliozzi, A.; Marchetti, P. *Nano Lett.* **2006**, *6*, 1933–9.
(8) Wilson, J. T.; Cui, W. X.; Chaikof, E. L. *Nano Lett.* **2008**, *8*, 1940–8.
(9) Veerabadran, N. G.; Goli, P. L.; Stewart-Clark, S. S.; Lvov, Y. M.; Mills, D. K. *Macromol. Biosci.* **2007**, *7*, 877–82.
(10) Miura, S.; Teramura, Y.; Iwata, H. *Biomaterials* **2006**, *27*, 5828–35.
(11) De Geest, B. G.; De Koker, S.; Sukhorukov, G. B.; Kreft, O.; Parak, W. J.; Skirtach, A. G.; Demeester, J.; De Smedt, S. C.; Hennink, W. E. *Soft Matter* **2009**, *5*, 282–91.
(12) Decher, G. *Science* **1997**, *277*, 1232–7.
(13) Jones, P. M.; Courtney, M. L.; Burns, C. J.; Persaud, S. J. *Drug Discovery Today* **2008**, *13*, 888–93.
(14) Efrat, S. *Adv. Drug Delivery Rev.* **2008**, *60*, 114–23.
(15) Lai, Y.; Drobinskaya, I.; Kolossov, E.; Chen, C.; Linn, T. *Adv. Drug Delivery Rev.* **2008**, *60*, 146–59.
(16) Phillips, M. I.; Tang, Y. J. *Adv. Drug Delivery Rev.* **2008**, *60*, 160–72.
(17) Ishihara, H.; Asano, T.; Tsukuda, K.; Katagiri, H.; Inukai, K.; Anai, M. *Diabetologia* **1993**, *36*, 1139–45.
(18) Aoki, T.; Hui, H.; Umehara, Y.; LiCalzi, S.; Demetriou, A. A.; Rozga, J.; Perfettit, R. *Cell Transplant.* **2005**, *14*, 411–21.
(19) Barrientos, R.; Baltrusch, S.; Sigrist, S.; Legeay, G.; Belcourt, A.; Lenzen, S. *Horm. Metab. Res.* **2009**, *41*, 5–9.
(20) Carvell, M.; Persaud, S. J.; Jones, P. M. *Cell Sci. Rev.* **2006**, *3*, 100–28.
(21) Hauge-Evans, A. C.; Squires, P. E.; Persaud, S. J.; Jones, P. M. *Diabetes* **1999**, *48*, 1402–8.
(22) Halban, P. A.; Powers, S. L.; George, K. L.; Bonner-Weir, S. *Diabetes* **1987**, *36*, 783–90.
(23) Miyazawa, K.; Winnik, F. M. *Macromolecules* **2002**, *35*, 9536–9544.
(24) Jones, K. H.; Senft, J. A. *J. Histochem. Cytochem.* **1985**, *33*, 77–9.
(25) Gey, G. O.; Gey, M. K. *Am. J. Cancer* **1936**, *27*, 45–76.
(26) Jones, P. M.; Salmon, D. M.; Howell, S. L. *Biochem. J.* **1988**, *254*, 397–403.
(27) Mano, J. F.; Silva, G. A.; Azevedo, H. S.; Malafaya, P. B.; Sousa, R. A.; Silva, S. S. *J. R. Soc. Interface* **2007**, *4*, 999–1030.
(28) Jiang, T.; Kumbar, S. G.; Nair, L. S.; Laurencin, C. T. *Curr. Top. Med. Chem.* **2008**, *8*, 354–64.
(29) de Vos, P.; Faas, M. M.; Strand, B.; Calafiore, R. *Biomaterials* **2006**, *27*, 5603–17.
(30) Nakaya, T.; Li, Y. J. *Des. Monomers Polym.* **2003**, *6*, 309–51.
(31) Porcel, C.; Lavalle, Ph.; Decher, G.; Senger, B.; Voegel, J.-C.; Schaaf, P. *Langmuir* **2007**, *23*, 1898–904.
(32) Zhi, Z.-L.; Haynie, D. T. *Macromolecules* **2004**, *37*, 8668–75.
(33) Boyd, A. S.; Wood, K. J. *Transplantation* **2009**, *87*, 1300–4.
(34) Yaney, G. C.; Fairbanks, J. M.; Deeney, J. T.; Korchak, H. M.; Tornheim, K.; Corkey, B. E. *Am. J. Physiol. Endocrinol. Metab.* **2002**, *283*, 880–8.
(35) Hatlapatka, K.; Willenborg, M.; Rustenbeck, I. *Am. J. Physiol. Endocrinol. Metab.* **2009**, *297*, E315−E322.

BM901152K